Experimental study of woods under external heat flux by autoignition

Ignition time and mass loss rate

Long Shi · Michael Yit Lin Chew

Abstract Piloted ignition of woods has been commonly investigated, which is accelerated by a spark plug. Autoignition is a complex phenomenon that combustible materials are ignited by internal heating, without the spark plug. Compared with piloted ignition, process of autoignition is closer to the development of real fire. Very few studies have focused on the prediction of ignition time and average mass loss rate by autoignition. Therefore, ignition time and mass loss rate on six species of commonly used wood samples, namely pine, beech, cherry, oak, maple, and ash, were studied under external heat flux by autoignition in a cone calorimeter. Three mass loss stages of woods under external heat flux was observed. Empirical models of ignition time and average mass loss rate for woods under external heat flux were developed. These empirical models can be used not only for fire risk evaluation, but also for modeling input and validation.

Keywords Autoignition · Ignition time · Ignition temperature · Mass loss rate · Cone calorimeter

Introduction

Ignition tends to mean two different things [1]: (1) kindled ignition where a body is ignited by an external heat source such as flame, sparks or hot surface, and in general, measurement of ignition point based on the American Society for Testing and Materials (ASTM) is widely used; and (2) autoignition (or spontaneous ignition, self-ignition, non-flaming ignition) where certain combustible materials can be ignited as a result of internal heating which arises spontaneously if there is an exothermic process liberating heat faster than it can be lost to the surrounding. Most of previous studies focused on the kindled ignition.

Although kindled ignition is very common, it is not instrumented to account for flow effects, in-depth radiation effects and ambiguities resulting from the emission spectral characteristics of material and heat flux source [2]. Prediction models developed previously are used to predict ignition time or average mass loss rate of woods by piloted ignition.

Compared with piloted ignition, process of autoignition is closer to the development of real fire. But very few studies have focused on the prediction of ignition time and average mass loss rate by autoignition. No empirical model has been found about the prediction of ignition time and average mass loss rate of woods by autoignition. Blijderveen et al. [3] obtained that the autoignition behavior is determined by a combination of convective heat transfer between primary air flow and fuel bed and heat gained by reactions in the fuel bed. And the heat gained by reactions is determined by exothermic hemicelluloses pyrolysis. Wang et al. [4] analyzed the influence of ambient pressure and oxygen content on autoignition by conducting contrastive experiments at two different altitudes. Results showed that mass loss rate of wood at high altitudes (3,650 m) is higher than the one at low altitudes (50 m), while ignition delay time of the sample at high altitude is shorter. Liodakis et al. [5] studied autoignition delay times of some Mediterranean forest species. Results showed that ignitability depends mainly on the amount of cellulose decomposed during pyrolysis, as well as on the total mass residue after thermal treatment up to 600 °C.

L. Shi (✉) · M. Y. L. Chew
Department of Building, National University of Singapore,
4 Architecture Drive, Singapore 117566, Singapore
e-mail: shilong@mail.ustc.edu.cn; shilong@nus.edu.sg

Experimental study of six species of woods were conducted under external heat flux by autoignition. The objectives of this study are:

- To obtain an appropriate model for the prediction of ignition time of woods by autoignition;
- To gain a model for predicting average mass loss rate when wood is under external heat flux by autoignition; and
- To provide input parameters or validation data for numerical models describing fire behaviors of woods under external heat flux by autoignition.

Methodology

Materials

Measured properties of wood samples are listed in Table 1. The sample sizes are 100×100 mm with different thicknesses, such as 10, 20, and 30 mm.

Samples were put under ambient environment for more than 24 h. Moisture contents of wood samples were then measured according to the oven-dry method [6] by chamber furnace. In the furnace, temperature inside kept at a range of 102–105 °C to drop off the moisture inside the wood slabs. Periodical re-weighing were taken until no further weight loss was registered. The moisture content (wet basis) provided in Table 1 are the average of three different thicknesses.

Apparatus

Cone calorimeter [7–10] as a frequent used equipment for piloted or autoignition experiments was used in this study. Wood samples were put in horizontal orientation on specimen holder. External heat fluxes of 25, 50, and 75 kW m^{-2} were chosen for this study.

Thermocouples were used to measure temperature at surface and different depths of wood slab. Type-N thermocouples with wire thickness of 0.8 mm were imbedded into the samples horizontally. For 20 mm thickness wood samples, thermocouples were placed every 5 mm from surface to the bottom. And for 30 mm thickness samples thermocouples were posited every 5 mm from surface to 25 mm depth. Thermocouples for 10 thickness wood samples were placed at surface and depths of 3, 6, and 10 mm (bottom).

Procedure

Before experiments, gas analyzers and external heat flux were first calibrated accordingly. Wood samples were then secured on a specimen holder and placed under the heater horizontally. The edges and rear surface of the specimens were covered with aluminum foil for insulation. Change in weight was dynamically recorded using the build-in weighting device. Temperatures at surface and different depths of wood samples were recorded using a data logger. A sample was considered ignited when visible flame was first observed. Surface temperature at ignition was considered as the ignition temperature. Spark plug was not used during the whole experimental time.

Results and discussion

Thermal degradation

The main chemical components of woods are cellulose, hemicelluloses, and lignin. According to Janssens and Douglas [11], these three main components have quite different thermal degradation characteristics, showing that the constituents decompose to release volatiles over different temperature ranges. The cellulose decomposes in a temperature range of 240–350 °C, hemicelluloses in a range of 200–260 °C, and lignin in a range of 280–500 °C.

Figure 1 shows mass loss stages of wood under 25 kW m^{-2} heat flux. The surface and bottom temperature of wood samples are provided associated with mass loss rate. Under external heat, surface temperature will rise first, and bottom temperature start to rise when heat reaches the

Table 1 Measured properties of wood samples

Species	Material	Grain orientation	Average density/kg m^{-3}	Average moisture content/%
Softwood	Pine (*Pinus contorta*)	Along	446.8	12.1
Hardwood	Beech (*Fagus grandifolia*)	Along	632.4	10.4
	Cherry (*Prunus serotina*)	Along	557.6	11.3
	Oak (*Quercus rubra*)	Along	897.3	10.4
	Maple (*Acer nigrum*)	Along	748.2	10.0
	Ash (*Fraxinus americana*)	Along	680.0	10.2
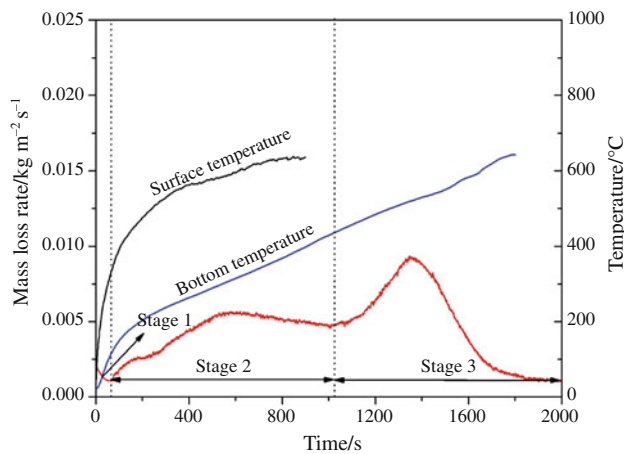
Fig. 1 Mass loss stages of cherry under 25 kW m^{-2} external heat flux
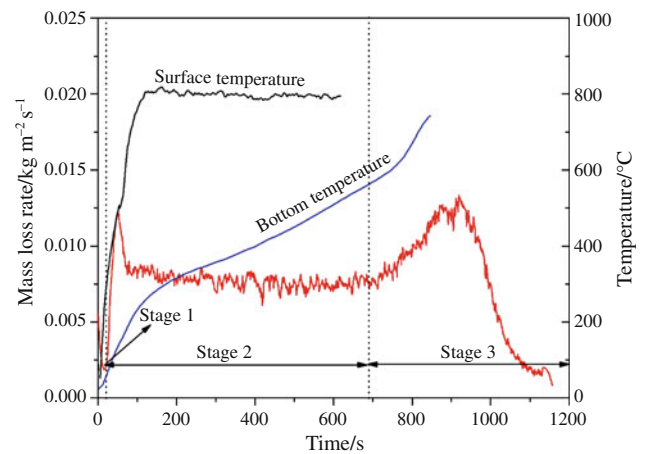
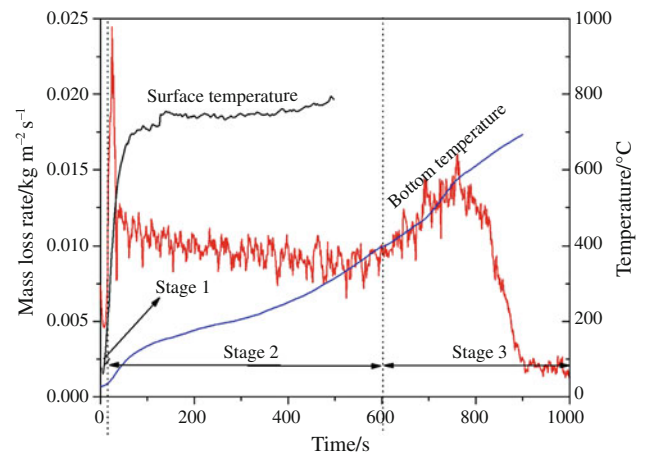Fig. 2 Mass loss stages of cherry under 50 kW m^{-2} external heat flux

Fig. 3 Mass loss stages of cherry under 75 kW m^{-2} external heat flux

bottom. When temperature is rising, the surface temperature can be considered the highest temperature inside the whole wood slab, and bottom temperature as the lowest temperature. To determine temperature range of a stage, it may can be considered that the stage starts at surface temperature and ends at bottom temperature.

According to peak mass loss rate, three mass loss stages can be observed. The first stage of mass loss is due to water evaporation. As analyzed above, temperature range of this stage is 20–110 °C. Temperature range of second stage is about 110–440 °C. It is known that cellulose, hemicelluloses, and lignin decompose at this stage. The third stage when temperature is higher than 440 °C may be the decomposition reaction of remaining lignin and char.

Figure 2 shows mass loss stages of wood under 50 kW m^{-2} heat flux. Similarly, three mass loss stages can be observed. The temperature ranges of first three stages are 20–65, 65–550, and 550 °C above, respectively. Temperature is lower than 100 °C at the end of the first stage. This may indicate that not all the water has evaporated during this stage because of a short time of 18s. And then comes to the second stage of decomposition of cellulose and hemicelluloses.

Figure 3 shows mass loss stages of wood under 75 kW m^{-2} heat flux. Three mass loss stages also can be observed. Temperature ranges of three stages are 20–40, 40–400, and 400 °C above, respectively. Temperature is also lower than 100 °C at the end of the first stage. Same reason may can be addressed for this phenomenon. As mentioned-above, cellulose and hemicelluloses decompose at temperature range of 240–350 and 200–260 °C, respectively. Decomposition starting temperature of cellulose and hemicelluloses are very low. The reason why the first two stages are close may be because of the temperature inside the wood slab which increases dramatically under high

external heat flux, then water evaporation and the decomposition of cellulose and lignin happen almost at the same time.

According to the peak mass loss rate, three mass loss stages can be observed. The first stage is the water evaporation. The second stage is the decomposition of cellulose, hemicelluloses, and lignin. The first two stages are getting closer when external heat flux is higher. This may be because of the temperature inside the wood slab which increase dramatically under high external heat flux, and water evaporation and decomposition of cellulose and lignin happen almost at the same time. For the third stage, start temperatures of 25, 50, 75 kW m^{-2} external heat flux are 440, 550, and 400 °C, respectively. As in the Eurocode 5 [12], char depth was considered to be located at the 300 °C isotherm inside wood slab. When the third stage begins, temperatures inside the whole wood slab are higher

Table 2 A summary of previous models to predict piloted ignition time

Model	Equation	Assumption
Quintiere [13]	$t_{ig} \approx \frac{2}{3} \lambda \rho C_p \left(\frac{T_{ig} - T_0}{\dot{q}''} \right)^2$	–Ignition occurs when surface temperature achieves critical value; Solid is inert up to ignition; and Solid is infinitely thick
Atreya and Abu-Zaid [14]	$t_{ig} = \frac{\pi}{4} \lambda \rho C_p \left(\frac{T_{ig} - T_0}{\dot{q}''} \right)^2$	–No heat losses; and Surface temperature at ignition is assumed to be a constant
Mikkola and Wichman [15]	$\begin{cases} t_{ig} = \rho C_p L \frac{T_{ig} - T_0}{\dot{q}''} & \text{(Thermal thin)} \\ t_{ig} = \frac{\pi}{4} \lambda \rho C_p \left(\frac{T_{ig} - T_0}{\dot{q}''} \right)^2 & \text{(Thermal thick)} \end{cases}$	–Heat losses from the sample surface are linearized
Delichatsios et al. [2]	$\begin{cases} t_{ig} = \frac{1}{\pi} \lambda \rho C_p \left(\frac{T_{ig} - T_0}{\dot{q}'' - \dot{q}''_{cr}} \right)^2 & (\dot{q}'' < 1.1 \dot{q}''_{cr}) \\ t_{ig} = \frac{\pi}{4} \lambda \rho C_p \left(\frac{T_{ig} - T_0}{\dot{q}'' - 0.64 \dot{q}''_{cr}} \right)^2 & (\dot{q}'' > 3 \dot{q}''_{cr}) \end{cases}$	–The materials is thermally thick, and the thickness may be considered to be infinite; and Reradiation losses are ignored in the analysis
Carslaw and Jaeger [16]	$t_{ig} = \frac{\pi}{4} \lambda \rho C_p \left(\frac{T_{ig} - T_0}{\varepsilon \dot{q}''} \right)^2$	–Thermally thick materials
Harada [18]	$t_{ig} = 14.4 \frac{\lambda \rho C_p}{\dot{q}''^3} + 8.64$	–Empirical equation from experiments
Babrauskas [19, 20]	$t_{ig} = \frac{130 \rho^{0.73}}{(\dot{q}'' - 11.0)^{1.82}}$	–Empirical equation by correlation of literature data

Note symbols in these equations are: t_{ig} is the ignition time, s; T_{ig} is the ignition temperature, °C; T_0 is the ambient temperature, °C; λ is the thermal conductivity, kW m^{-1} °C^{-1}; ρ is the density, kg m^{-3}; C_p is the specific heat capacity, kJ kg^{-1} °C^{-1}; $\dot{q}''$ is the external heat flux, kW m^{-2}; L is the thickness of woods, mm; $\dot{q}''_{cr}$ is the critical heat flux, kW m^{-2}; and ε is the emissivity

than 300 °C, indicating that the whole wood slab has changed into char. So it may be gained that still there is a peak mass loss rate when all the wood changes into char.

Ignition time

Substantial amount of work have been done regarding the prediction models for piloted ignition. Two kinds of approaches are used to develop these models. The first one is formula deduction. Quintiere [13] gained an approximate solution of ignition time by solving integral equations. It was assumed that ignition is based on critical temperature of surface under external heat flux. The ignition time was found to be related with thermal inertia, ignition temperature, and external heat flux. Atreya and Abu-Zai [14] obtained a similar result with a different coefficient for the correlation. Others influencing factors were also considered in previous models, such as thermal thickness [15], range of external heat flux [2], and emissivity [16, 17]. The other approach is correlation using experimental data. Harada [18] found a linear correlation between ignition time and thermal inertia of wood samples by piloted ignition. And Babrauskas [19, 20] gained a linear relationship between ignition time and other factors, such as density and external heat flux. A summary of previous models for piloted ignition time are listed in Table 2.

From previous models, shown in Table 2, it is known that ignition time may be related with some wood's properties or environmental factors, such as thermal inertia, thickness, external heat flux, critical heat flux, or emissivity.

By making calculations for various densities and heat fluxes, a minimum thickness for particle board required to insure that the specimen is thermal thick can be represented by [21]:

$$L = 0.6 \frac{\rho}{\dot{q}''} \qquad (1)$$

where L is the thickness of specimen, mm; ρ is density, kg m^{-3}; and $\dot{q}''$ is the external heat flux, kW m^{-2}.

Quintiere [13], Atreya and Abu-Zaid [14] obtained a similar result that ignition time is linear with $\lambda \rho C_p [(T_{ig} - T_0)/\dot{q}'']^2$. The coefficient in Quintiere's equation is 2/3, and $\pi/4$ in Atreya and Abu-Zaid's equation. Carslaw and Jaeger's equation [16] is similar to these two under a consideration of woods' emissivity. The influence of emissivity to ignition time may be ignored under this circumstance because they are almost identical for these wood samples [22]. In this way, these equations mentioned above belong to one type, which can be expressed as:

$$t_{ig} = a_1 \cdot \lambda \rho C_p \left(\frac{T_{ig} - T_0}{\dot{q}''} \right)^2 \qquad (2)$$

where t_{ig} is the ignition time, s; a_1 is the coefficient in the correlation; λ is the thermal conductivity, kW m^{-1} °C^{-1}; C_p is the specific heat capacity, kJ kg^{-1} °C^{-1}; T_{ig} is the

ignition temperature, °C; and T_0 is the ambient temperature, °C.

Mikkola and Wichman [15] obtained an equation to predict piloted ignition time for thermal thick or thermal thin specimens. Densities of specimens in this study are between 446 kg m^{-3} and 898 kg m^{-3}. And external heat flux of 25, 50, and 75 k Wm^{-2} were chosen. For specimen under 25 kW m^{-2} heat flux, shown in the following section, no visible flame was observed during the whole experimental time. According to Eq. (1), it is known that almost all the specimens under 50 and 75 kW m^{-2} external heat flux are thermal thick, except oak when it is positioned under 50 kW m^{-2} heat flux. For thermal thick specimens, Mikkola and Wichman's equation can also be expressed by Eq. (2).

For equation from Delichatsios et al. [2], external heat flux is considered as dependent condition. Ignition time correlates linearly with $\lambda \rho C_p [(T_{ig} - T_0)/(\dot{q}'' - \dot{q}''_{cr})]^2$ when external heat flux is less than 1.1 times of critical heat flux, and correlates with $\lambda \rho C_p [(T_{ig} - T_0)/(\dot{q}'' - 0.64\dot{q}''_{cr})]^2$ when external heat flux is higher than 3 time of critical heat flux. Mehaffey [23] gained a critical heat flux of woods of 28 kW m^{-2} for autoignition. So two equations may can be used to predict ignition time of autoignition, which are expressed as:

$$t_{ig} = a_2 \cdot \lambda \rho C_p \left(\frac{T_{ig} - T_0}{\dot{q}'' - 28.0} \right)^2 \tag{3}$$

$$t_{ig} = a_3 \cdot \lambda \rho C_p \left(\frac{T_{ig} - T_0}{\dot{q}'' - 18.0} \right)^2 \tag{4}$$

Another type of correlation is an empirical equation gained by Harada [18], showing that ignition time correlates linearly with $\lambda \rho C_p/\dot{q}''^3$, which can be expressed by:

$$t_{ig} = a_4 \cdot \frac{\lambda \rho C_p}{\dot{q}''^3} + b_4 \tag{5}$$

Based on literature data gained in the cone calorimeter, a correlation was developed by Babrauskas [19, 20]. The correlation were sought on the basis of capturing density, moisture, and orientation (horizontal and vertical) effects, with data available on densities over a range of 170–850 kg m^{-3}. It was found that piloted ignition time of wood correlates linear with $\rho^{0.73}/(\dot{q}'' - 11.0)^{1.82}$. In this equation, for piloted ignition, if $\dot{q}'' \rightarrow 11.0$, $t_{ig} \rightarrow \infty$. This means that the critical heat flux of wood by piloted ignition is about 11 kW m^{-2}. It is known from Mehaffey [23] that critical heat flux of wood by autoignition is about 28 kW m^{-2}. Therefore, for autoignition, if $\dot{q}'' \rightarrow 28.0$, $t_{ig} \rightarrow \infty$. Based on this, a type of correlation is assumed as:

Table 3 Ignition time and ignition temperature of wood samples

Material	Thickness/mm	50 kW m^{-2} heat flux		75 kW m^{-2} heat flux	
		Ignition time/s	Ignition temperature/°C	Ignition time/s	Ignition temperature/°C
Pine	10	61	558.2	23	348.6
	20	48	433.8	11	306.6
	30	27	433.1	12	314.0
Beech	10	46	370.6	20	338.0
	20	45	503.8	13	270.4
	30	39	370.6	18	378.9
Cherry	10	54	465.4	16	425.0
	20	57	543.6	11	334.4
	27	37	433.1	10	346.5
Oak	10	119	511.7	26	482.2
	20	79	453.5	24	353.7
	30	57	488.6	23	398.6
Maple	10	87	436.0	27	332.4
	20	87	491.1	26	399.2
	30	56	393.0	18	361.1
Ash	10	59	425.6	21	291.7
	20	57	487.6	19	340.9
	30	23	346	13	264.4

$$t_{ig} = a_5 \cdot \frac{\rho^{0.73}}{(\dot{q}'' - 28.0)^{1.82}} \qquad (6)$$

These five equations, namely Eqs. (2)–(6), will be used in the correlation to identify which one is appropriate for the prediction of ignition time by autoignition.

Table 3 shows ignition time and ignition temperature of six species of wood samples. For external heat flux of 25 kW m^{-2}, no visible flame was observed during whole experimental time, indicating that critical heat flux of these specimens is higher than 25 kW m^{-2}, which is much higher than those of piloted ignition. Mehaffey [23] gained that critical heat flux of wood by autoignition is about

28 kW m^{-2}. The range of ignition temperature is about 264–558 °C. Babrauskas [20] obtained that the range of ignition temperature for autoignition is 200–510 °C, which gave a little lower range of ignition temperature. Maybe this is because some of the experiments were conducted under lower external heat flux.

Thermal conductivity and specific heat of each species of wood samples can be found in References [24–28]. Figure 4 are gained accordingly based on Eqs. (2)–(6). In this study, it is assumed that ignition happens when surface temperature reaches ignition temperature. In these figures, except Eq. (5), non-intercept model were used for other four equations.

Fig. 4 Correlation between ignition time and influencing factors using Eqs. (2)–(6)
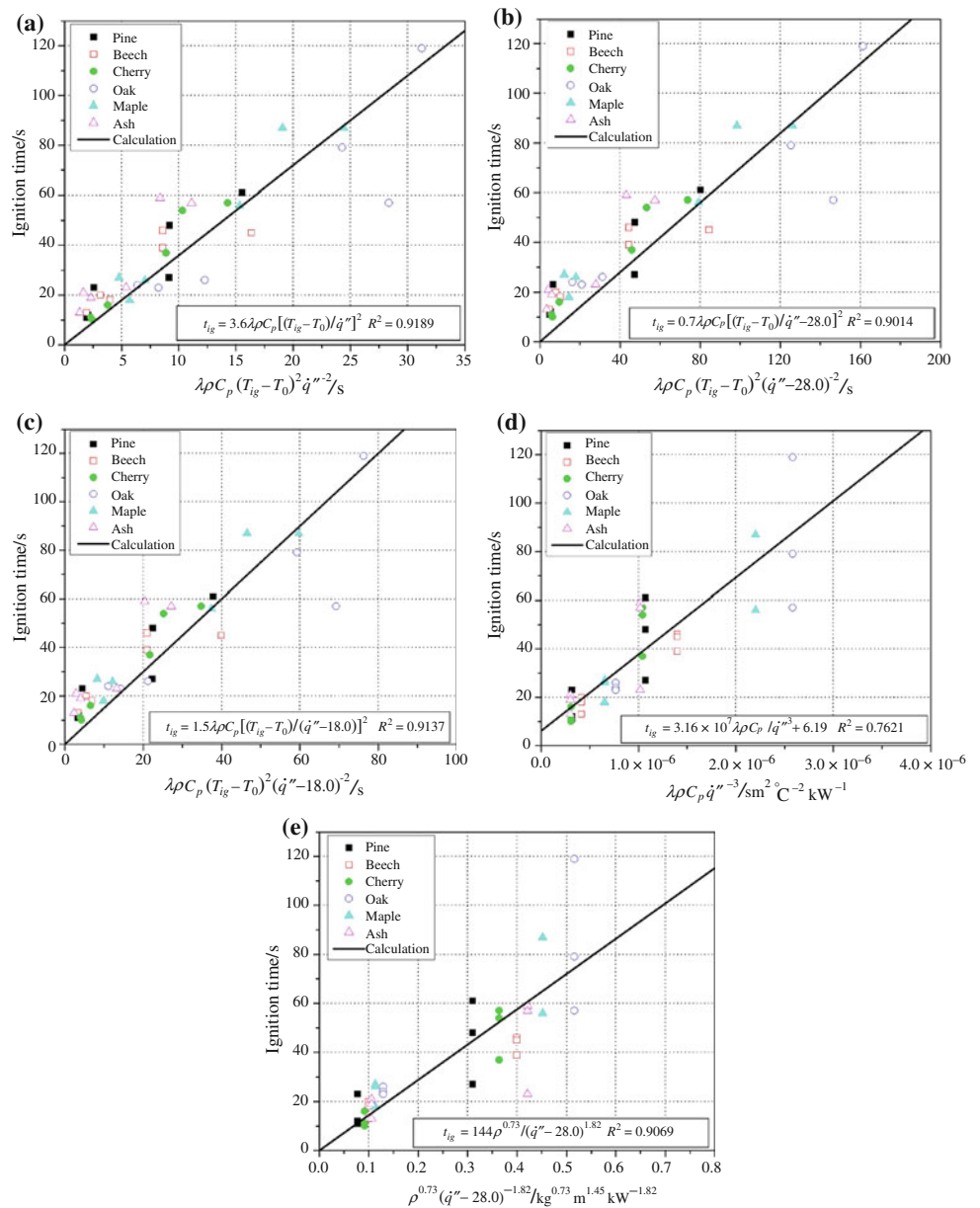
The values of R^2 for Eqs. (2)–(6) are 0.9189, 0.9014, 0.9137, 0.7621, and 0.9069, respectively. It is observed that R^2 value of Eqs. (2), (3), (4), and (6) are higher than 0.90. But in Eqs. (2), (3) and (4), ignition temperatures and thermal inertia are needed for prediction. It seems to be difficult to gain ignition temperature, especially for autoignition. For Eq. (6), only density and external heat flux, which are easy to be obtained, are needed for the prediction. Therefore, Eq. (6) is suggested to be used to predict ignition time of woods by autoignition:

$$t_{\text{ig}} = \frac{144\rho^{0.73}}{(\dot{q}'' - 28.0)^{1.82}}. \tag{7}$$

Mass loss rate

During experiments, thermocouples were used to measure temperature inside wood slab. Holes were drilled for emplacement of these thermocouple wires. Under the influences of thermocouple wires, some noises were produced in mass loss history data. Savitzky-Golay method [29] was used to solve this problem. This method optimally fits a set of data points to a polynomial in the least-squares sense, which has been developed and generalized well in the literatures. The main advantage of this method is that it tends to preserve features of the distribution such as relative maxima, minima, and width.

Branca and Di Blasi [30] obtained a range of about 65–85 % for weight loss of wood samples. It is very difficult to make an accurate comparison among average mass loss rates during whole experiment period because these woods vary in the final weight loss. To evaluate the mass loss rate well, an average mass loss rate (MLR$_{\text{ave}}$) from experiment start to 50 % mass loss is analyzed in this study.

A equation is assumed to examine the correlation between average mass loss rate and others factors, which is given as:

$$\text{MLR}_{\text{ave}} = \text{a} \cdot L^b \dot{q}''^c \rho^d \tag{8}$$

where MLR$_{\text{ave}}$ is the average mass loss rate from experiments start to 50 % mass loss, gm^{-2} s^{-1}.

Taking the logarithm of both sides, it is gained that:

$$\log \text{MLR}_{\text{ave}} = \log \text{a} + \text{b} \cdot \log L + \text{c} \cdot \log \dot{q}'' + \text{d} \cdot \log \rho \tag{9}$$

Coefficients a, b, c, and d are gained respectively by using linear regression method. The correlation between MLR$_{\text{ave}}$ and other factors such as thickness, external heat flux, and density is shown in Fig. 5. It is known that these two have a great linear correlation, which is given as:

$$\text{MLR}_{\text{ave}} = 0.016 L^{0.2} \dot{q}''^{0.8} \rho^{0.4} \tag{10}$$

For the t_{50}, it is gained that:

$$t_{50} = \frac{0.5 m_0}{\text{MLR}_{\text{ave}}} \tag{11}$$

where t_{50} is the time of 50 % mass loss, s; and m_0 is the original mass of specimen, s.

And it is known that MLR$_{\text{ave}}$ correlates linearly with $L^{0.2} \dot{q}''^{0.8} \rho^{0.4}$, and original mass correlates linearly with $L\rho$, so that:

$$t_{50} \propto \frac{L^{0.8} \rho^{0.6}}{\dot{q}''^{0.8}} \tag{12}$$

Fig. 6 shows a correlation between t_{50} and $L^{0.8} \rho^{0.6} / \dot{q}''^{0.8}$. These two show a good linear correlation, which is given as:
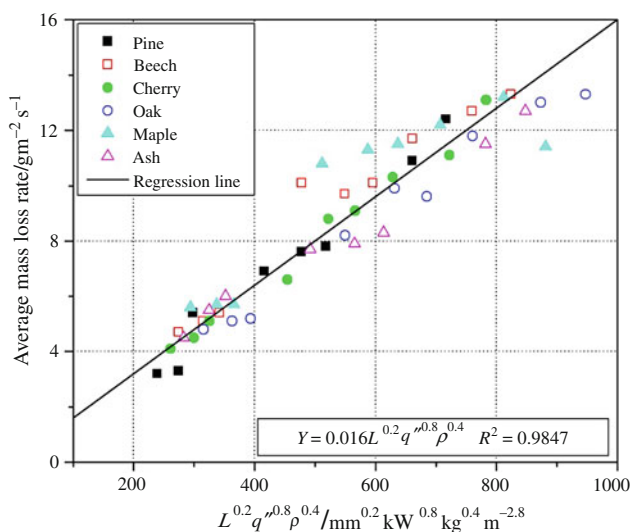

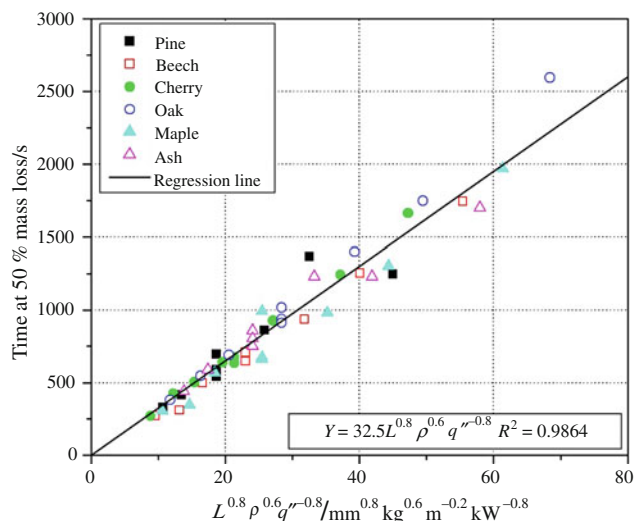Fig. 5 Correlation between average mass loss and other factors

Fig. 6 Correlation between time at 50 % mass loss and other factors

$$t_{50} = 32.5 \frac{L^{0.8} \rho^{0.6}}{\dot{q}''^{0.8}} \qquad (13)$$

Conclusions

Six species of wood samples, namely pine, beech, cherry, oak, maple, and ash, were studied experimentally under external heat flux by autoignition. The following conclusions can be addressed:

(1) Due to peak mass loss rate, degradation process of woods under external heat can be divided into three stages. The first stage is water evaporation, cellulose, hemicelluloses, and lignin decompose in the second stage, and degradation of remaining lignin and char happen in the third stage. Start temperatures of the third stage is higher than 300 °C, indicating that a peak mass loss rate exist after all wood slab changing into char.

(2) For autoignition, a range of ignition temperature of about 264–558 °C is obtained in this study. Results show a very good prediction of ignition time by density and external heat flux, which can be expressed by:

$$t_{ig} = \frac{144 \rho^{0.73}}{(\dot{q}'' - 28.0)^{1.82}} \qquad \text{(Thermal thick)}$$

(3) Average mass loss rate from experiment start to 50 % mass loss can be gained by thickness, external heat flux, and density:

$$\text{MLR}_{ave} = 0.016 L^{0.2} \dot{q}''^{0.8} \rho^{0.4} \qquad (10 \leq L \leq 30)$$

(4) The time at 50 % mass loss also can be obtained by woods' properties and environmental factors, which is given by:

$$t_{50} = 32.5 \frac{L^{0.8} \rho^{0.6}}{\dot{q}''^{0.8}} \qquad (10 \leq L \leq 30).$$

These empirical equations and data in this study not only can be used to predict ignition time, average mass loss rate of woods under external heat flux by autoignition, but also could provide input parameters for numerical modeling or be used for modeling validation.

References

1. Li XR, Koseki H, Momota M. Evaluation of danger from fermentation-induced autoignition of wood chips. J Hazard Mater. 2006;135:15–20.
2. Delichatsios MA, Panagiotou TH, Kiley F. The use of time to ignition data for characterizing the thermal inertia and the minimum (critical) heat flux for ignition or pyrolysis. Combust Flame. 1991;84:323–32.
3. Blijderveen MV, Gucho EM, Bramer EA, Brem G. Autoignition of wood, char and RDF in a lab scale packed bed. Fuel. 2010;89:2393–404.
4. Wang YF, Yang LZ, Zhou XD, Dai JK, Zhou YP, Deng ZH. Experiment study of the altitude effects on autoignition characteristics of wood. Fuel. 2010;89:1029–34.
5. Liodakis S, Bakirtzis D, Lois E. TG and autoignition studies on forest fuels. J Therm Anal Calorim. 2002;69:519–28.
6. Mitchell P. Methods of moisture content measurement in the lumber and furniture industries. www.ces.ncsu.edu/ (2011). Accessed 7 Mar 2012.
7. Fire Testing Technology Limited. User's guide for the cone calorimeter. West Sussex: Fire Testing Technology Limited; 2001.
8. Kim JY, Lee JH, Kim SM. Estimating the fire behavior of wood flooring using a cone calorimeter. J Therm Anal Calorim. 2011;. doi:10.1007/s10973-011-1902-1.
9. Xu Q, Griffin GJ, Jiang Y, Preston C, Bicknell AD, Bradbury GP, et al. Study of burning behavior of small scale wood crib with cone calorimeter. J Therm Anal Calorim. 2008;91:787–90.
10. Nie SB, Liu XL, Wu K, Dai GL, Hu Y. Intumescent flame retardation of polypropylene/bamboo fiber semi-biocomposites. J Therm Anal Calorim. 2012;. doi:10.1007/s10973-012-2422-3.
11. Janssens M, Douglas B. Wood and wood products. In: Harper CA, editor. Handbook of building materials for fire protection. New York: McGraw-Hill; 2004. p. 7.1–7.58.
12. Cachim PB, Franssen JM. Comparison between the charring rate model and the conductive model of Eurocode 5. Fire Mater. 2009;33:129–43.
13. Quintiere JG. A semi-quantitative model for the burning rate of solid materials. NISTIR 4840. Gaithersburg: National Institute of Standard Technology (NIST); 1992.
14. A. Atreya, M. Abu-Zaid, Effect of environmental variables on piloted ignition. *The 3rd international symposium on fire safety science*, University of Edinburgh, Scotland, 8–12 July 1991.
15. Mikkola E, Wichman IS. On the thermal ignition of combustible materials. Fire Mater. 1989;14:87–96.
16. Carslaw HS, Jaeger JC. Conduction of heat in solids. Oxford: The Clarendon Press; 1959.
17. M. Janssens, Fundamental thermo physical characteristics of wood and their role in enclosure fire growth. PhD Thesis, University of Gent, Belgium, 1991.
18. Harada T. Time to ignition, heat release rate and fire endurance time of wood in cone calorimeter test. Fire Mater. 2001;25:161–7.
19. Babrauskas V. Ignition handbook: principles and applications to fire safety engineering, fire investigation, risk management and forensic science. Issaquah: Fire Science Publishers; 2003.
20. Babrauskas V. Ignition of wood: a review of the state of the art. The ninth Interflam, Edinburgh. Scotland: Interscience Communications; 2001.
21. Babrauskas V, Parker WJ. Ignitability measurements with the cone calorimeter. Fire Mater. 1987;11:31–43.
22. Wesson HR, Welker JR, Sliepcevich CM. The piloted ignition of wood by thermal radiation. Combust Flame. 1971;16:303–10.
23. Mehaffey J. Fire dynamics I: ignition and burning of solids, Lecture notes. Ottawa: Carleton University; 2002.
24. W. Simpson, A. TenWolde, Physical properties and moisture relations of wood. In: Wood handbook—wood as an engineering material, Forest Products Laboratory, Madison 1999, pp 3.1–3.24.
25. The Engineering ToolBox. Solids—Specific heats. www.engineeringtoolbox.com/ 2011. Accessed 7 Mar 2012.
26. VanderGheynst JS, Walker LP, Parlange JY. Energy transport in a high-solids aerobic degradation process: mathematical modeling and analysis. Biotechnol Prog. 1997;13:238–48.

27. Hrcka R. Variation of thermal properties of beech wood in the radial direction with moisture content and density. The 6th international symposium wood structure and properties, Arbora Publishers, Zvolen, 2010.

28. Zahirovic S, Scharler R, Obernberger I. Advanced CFD modeling of pulverised biomass combustion. International conference on science in thermal and chemical biomass conversion, Victoria, Canada, 2004.

29. Luo JW, Ying K, Bai J. Savitzky-Golay smoothing and differentiation filter for even number data. Signal Process. 2005;85:1429–34.

30. Branca C, Di Blasi C. Global kinetics of wood char devolatilization and combustion. Energy Fuels. 2003;17:1609–15.